Hydride Precipitation Behavior in $\alpha+\beta$ Ti-6Al-4V Alloy†

Toshio ENJO* and Toshio KURODA**

Abstract

An investigation has been made into the hydrogen diffusion and hydrides precipitation behavior of $\alpha+\beta$ Ti-6Al-4V alloy by means of X-ray diffraction method, internal friction measurement and transmission electron microscopy.

The hydrogenation was made by cathodic charging at current densities of 50 A/m², 500 A/m² and 4200 A/m².

As the alloy was hydrogen-charged, the peak of α phase by X-ray diffraction line profile was hardly shifted, but that of β phase was shifted to the low angle side. d_{200} spacing of β phase increased with increasing the charging time and then became constant value.

It means that hydrogen was mainly diffused to the β phase and then solutionized to the solubility limit. This tendency was corresponded to the peak at about 80 K in the internal friction curves. And the peak at 80 K was clear to be Snoek peak.

Before charging, X-ray diffraction line profile showed only α phase and β phase peak. The new peak occurred at $2\theta = 60.9\ (\pi/180)$ rad., $92.8\ (\pi/180)$ rad. so on, as the alloy was cathodically charged. The peak height increased with increasing the hydrogen-charging time, and increasing the charging current density. It means that the peak is due to the hydride precipitation.

On the basis of X-ray diffraction line profiles, the volume fraction of α phase decreased with increasing the volume fraction of the hydrides, though that of β phase hardly changed, in the case of low current density of cathodic charging. It was confirmed by transmission electron microscopy. But in the case of high current density, both volume fraction of α phase and that of β phase decreased with increasing that of hydrides. It means that hydrides precipitated both in the α phase at α/β interface, and in the β phase. It was confirmed by transmission electron microscopy.

KEY WORDS: (Titanium Alloy) (Hydride) (Internal Friction Measurement) (Transmission Electron Microscopy) (Snoek Peak) (Hydride Peak)

1. Introduction

$\alpha+\beta$ Ti-6Al-4V alloy occurs the delayed cracking due to hydrogen induced cracking under tension stress such as residual stress in the environment of air and hydrogen, if the alloy has sharp microcracks such as weld cracks and machine work's cracking[1)–3)]. And the hydride plays an important role in the hydrogen induced cracking[4), 5)].

But the microscopic behavior of hydrogen and the precipitation behavior of the hydrides have not been clear yet.

α phase consists of hcp structure and β phase consists of bcc structure. Generally the critical solubility of hydrogen in the β phase is much higher than that of α phase, and the diffusivity of hydrogen in the β phase is much faster than that of α phase[6), 7)]. Hence the β phase network may act as a pipeline for transportation of hydrogen throughout the matrix, if the $\alpha+\beta$ alloy with crack were exposed in the hydrogen environment. And the hydride precipitation behavior may be also different from the α single phase such as commercially pure titanium (C.P.Ti).

The purpose of this paper is to present direct evidences for the precipitation of hydrides and absorption and diffusion of hydrogen in the $\alpha+\beta$ Ti-6Al-4V alloy cathodically charged at various current densities by means of X-ray diffraction technique, internal friction measurement and transmission electron microscopy.

2. Experimental Procedures

Ti-6Al-4V alloy was received in a mill annealed state. The thickness was 20 mm. The chemical compositions are shown in **Table 1**.

Table 1 Chemical compositions of Ti-6Al-4V alloy (wt%)

C	Fe	N	O	H	Al	V	Ti
0.011	0.204	0.0042	0.146	0.0045	6.26	4.15	Bal

† Received on October 31, 1984

* Professor

** Research Instructor

Transactions of JWRI is published by Welding Research Institute of Osaka University, Ibaraki, Osaka 567, Japan

The material was machined into specimens for X-ray diffraction techniques and internal friction measurement respectively, as shown in **Fig. 1**. The specimen surface was

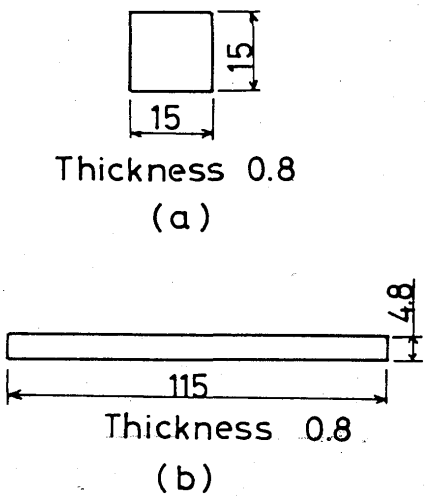

Fig. 1 Specimen geometries for X-ray diffraction method (a) and internal friction measurement (b)

finished using aceton after the polishing by emery paper of number of 1500 before the tests.

Hydrogenation was carried out using cathodic charging method in a $5\%H_2SO_4$ aqueous solution. The cathodic charging was made at 4200 A/m^2, 500 A/m^2, 50 A/m^2 respectively, in order to change the surface hydrogen concentration of the specimen.

X-ray line profiles were made by using X-ray diffractometer with copper radiation filtered by Ni.

To obtain the X-ray line profiles, the diffractometer was set for medium resolution, and an angular scanning speed of 1 (π/180) rad./min. or 0.5 (π/180) rad./min.

Line breadth measurements were made on selected diffraction peak by determining the width of the peak at a position equal to half to the maximum intensity, and also measured the integrated intensity. All of the breadth measurements were corrected for K_α double separation and instrumental broadening.

The d spacings for these peaks were also determined by using the angular position of maximum peak intensity. All the specimens were measured at room temperature below 293 K.

The internal friction measurement was performed using an inverted torsion pendulum over a temperature range of 70 K to 300 K at a frequency of about 1 Hz in the heating rate at 0.02 K/sec, as shown in **Fig. 2**.

Transmission electron microscopy specimens were prepared by jet polishing in the electrolyte consisted of 56 ml of percloric acid, 230 ml of butyl alcohol, and 580 ml of metanol, after polishing up to 150 μm thick by emery paper of No. 1500. The electropolishing was

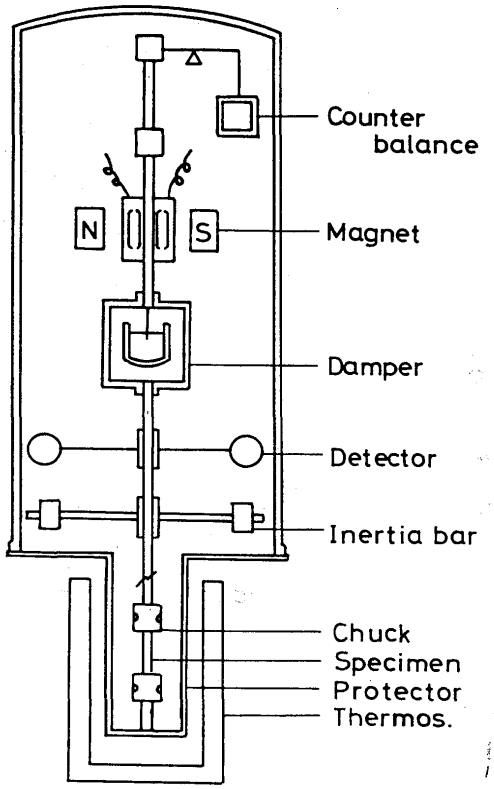

Fig. 2 Schematic diagram of internal friction measurement

performed at 14.5 V and below 233 K.

After the specimens were obtained, the specimens were immediately examined in a Hitachi HU-12A electron microscope at 125 KV.

3. Results and Discussion

3.1 Change in X-ray line profile by hydrogenation

Figure 3 shows the optical micrograph(a) and transmission electron micrograph of thin foil(b) for mill annealed specimen before cathodic charging.

For the optical micrograph, the mill annealed specimen consists of α phase observed as white platelets, and β phase observed as dark lines at the α/β interfaces. For transmission electron micrograph, α phase is deformed a little. The hydride is hardly observed.

Figure 4 indicates the X-ray line profiles of C.P.Ti and Ti-6Al-4V (mill annealed) alloy cathodic charging at 4200 A/m^2, for 18.8 ks respectively. For C.P.Ti, the peaks of γ hydride phase are observed at 59 (π/180) rad., 71 (π/180) rad., 74 (π/180) rad. and 99 (π/180) rad.. The angle due to hydride precipitation was corresponded to that of ASTM cards (9-371, 25-982, 25-983).

For Ti-6Al-4V alloy, the angle 2θ corresponded to the hydride phase shifts to a large angle side, comparing with

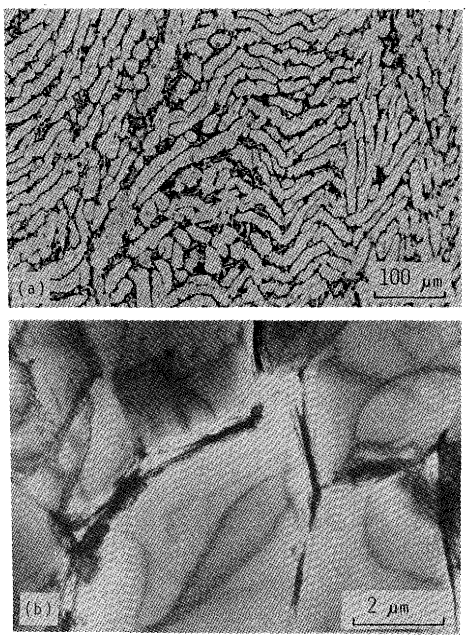

Fig. 3 Optical micrograph(a) and transmission electron micrograph of thin foil(b) for mill annealed specimen before charging

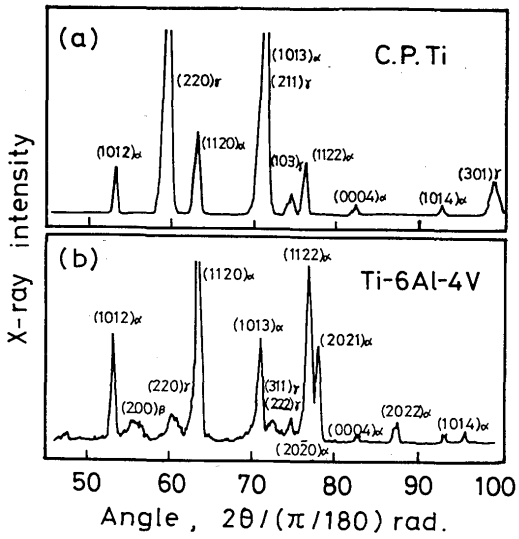

Fig. 4 X-ray diffraction patterns of commercially pure titanium (C.P.Ti)(a) and Ti-6Al-4V(b) hydrogen-charged at 4200 A/m^2 for 18.8 ks respectively

that of C.P.Ti. It is considered that the hydrides in Ti-6Al-4V alloy involves vanadium, which the atomic radius is smaller than that of titanium.

The peak by β phase is also observed at 57 (π/180) rad.. The line breadth also occurs by cathodic charging.

Then, the change in the X-ray diffraction profiles as the specimens were cathodically charged at various current densities for various charging times are shown in **Fig. 5**.

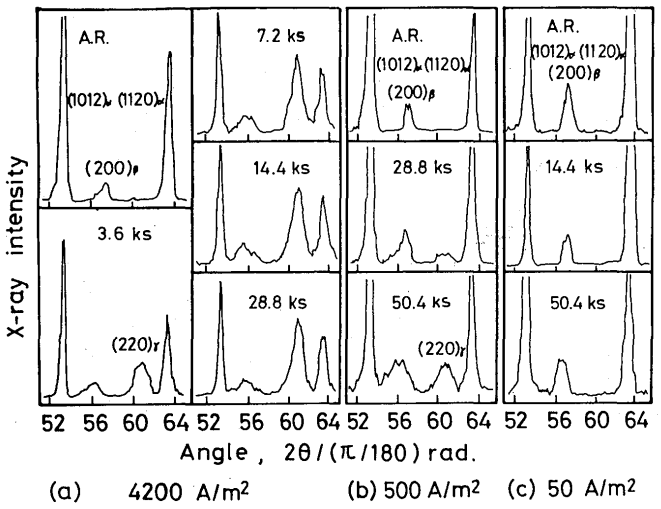

Fig. 5 X-ray diffraction patterns of Ti-6Al-4V alloy hydrogen-charged at various current densities for various times

The peak due to hydrides is hardly observed before charging for as-received state. But, for the hydrogenation at 4200 A/m^2, the γ hydride peak generates at 60.9 (π/180) rad. as the specimens were cathodic charged for 3.6 ks. And the integrated intensity of the peak increases with increasing the charging time.

For the hydrogenation of 500 A/m^2, γ (220) peak generates even if the charging time of 50.4 ks. Consequently, the current density is considered to decide the surface hydrogen concentration of the specimen.

Concerning the β phase, the diffraction line at (200) plane shifts a little toward the low angle side by hydrogenation even at any current density. But, that of α phase hardly shift at any current density.

Consequently, hydrogen is considered to absorb and diffuse to the β phase preferentially, as the hydrogenation was performed to the $\alpha+\beta$ microstructure.

3.2 Change in internal friction curves by hydrogenation

Figure 6 indicates the change in the internal friction curves of mill annealed Ti-6Al-4V alloy, as the specimens were cathodically charged at 4200 A/m^2 and 50 A/m^2 for various times.

The peak at about 80 K and the peak at 190 to 220 K increase with increasing the charging time at any current density.

For the peak at about 80 K, the peak is saturated and becomes constant by hydrogenation of short time at a high current density. The constant value is independent of the current density. This peak is hardly observed for the material which has not β phase, such as C.P.Ti consists of α phase, so the peak at about 80 K is considered to be related to the hydrogen content in the β phase.

The peak height at 190 K to 220 K increase with in-

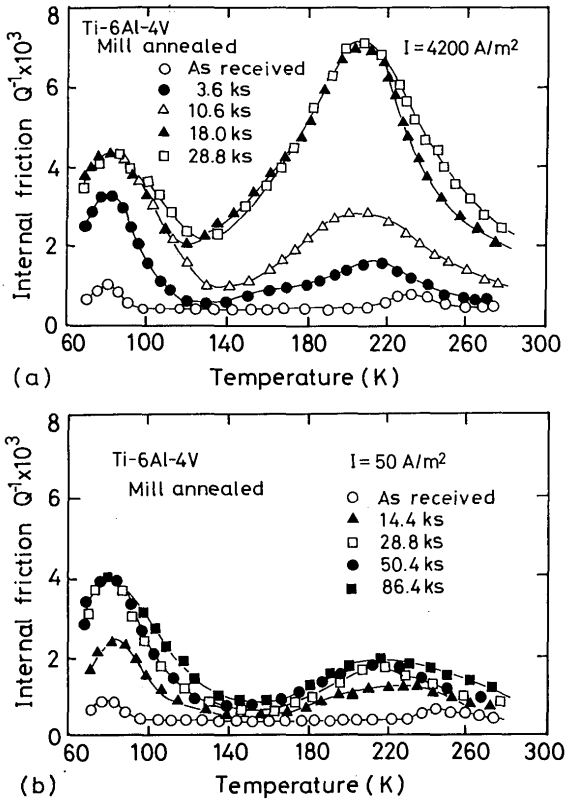

Fig. 6 Internal friction curves of Ti-6Al-4V alloy hydrogen-charged at 4200 A/m²(a) and 50 A/m²(b) for various times respectively

creasing the hydrogen charging time for the high current density. But, the peak height at 190 K to 220 K hardly increase with increasing the charging time for the low current density.

Consequently, this peak is considered to be related to the current density of cathodic charging. The peak is considered to be related to the the hydride precipitation, because that the peak is similar to the increase tendency of the hydride peak at 59 (π/180) rad. in the X-ray line profile shown in Fig. 5.

The peaks are also observed at 220 K to 260 K shown in Fig. 6-(a). This peak generates by the cathodic charging, which is also considered to be related to the hydride precipitation.

3.3 Solution behavior of hydrogen in the β phase.

As shown in Fig. 5, the diffraction peaks of α phase are hardly shifted, but that of β phase is shifted to the low angle side by cathodic charging. The X-ray line profile of the hydrogenated Ti-6Al-4V alloy showed that the absorbed hydrogen had a pronounced effect on the angular diffraction position and line breadth of the β phase peaks.

The intensity of the β (200) peak was sufficient to obtain quantitative data of the line breadth and d spacing. Therefore, these parameters were determined for the (200) β phase in all of the hydrogenated specimens.

Figure 7 indicates the relation between d_{200} spacing

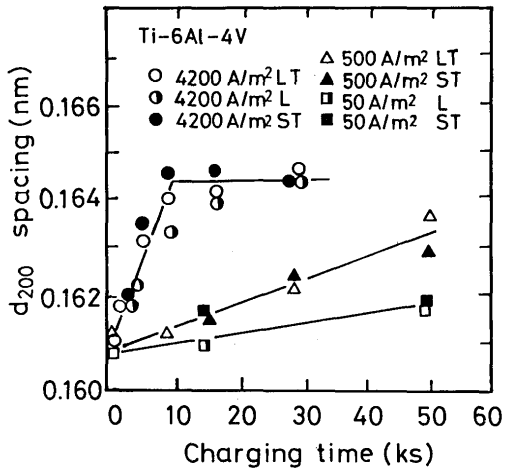

Fig. 7 Relation between d_{200} spacing of β phase and charging time by X-ray diffraction method

and charging time. The d_{200} spacing in the β phase also changed significantly as the hydrogen charging of the material increased.

A linear relationship appeared to exit between the d_{200} spacing and the charging time and reaches a maximum value of 0.1645 nm and remains at the relatively constant value.

This results mean that the β phase continued to absorb hydrogen and expanded up to a hydrogen level of 6000 ppm[7]. But, the d_{200} peak is not saturated yet at the low current density of hydrogen charging.

Figure 8 indicates the relation between peak height at about 80 K and charging time in the internal friction curves shown in Fig. 6. The peak height increases with increasing the charging time at any current density, and reaches a maximum value. For the low current density, the charging time reached a constant value is longer. The tendency of the results is resemble closely in the comparison between Fig. 7 and Fig. 8.

In this investigation, the hydrogen concentration gradient occurs in the specimen by cathodic charging. The information near the specimen surface can be obtained for X-ray diffraction method, but for the internal friction measurement, the information can be obtained not only from the specimen surface but also from the specimen inside.

The diffusivity of hydrogen in the β phase is much faster than that of α phase[13], and the solubility of hydrogen is much greater in the β phase than in the α phase[7], hence the β phase network can act as a pipeline for transportation of hydrogen throught the matrix during

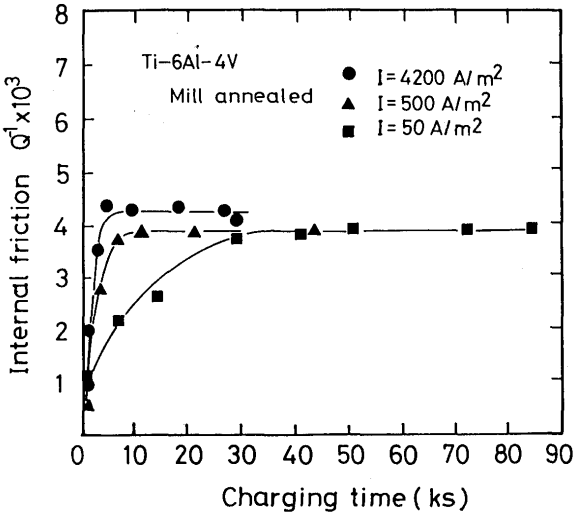

Fig. 8 Relation between peak height at 80 K and charging time by internal friction measurement

cathodic charging.

Based on the results, the peak at 80 K is considered to be Snoek peak of hydrogen in the β phase. If the peak is due to the Snoek peak, the activation energy is considered to become the value of 20000 J/mol, which is activation energy for hydrogen diffusion in the β phase[13].

For the evaluating the activation energy using internal friction measurement, it is well known to be two kinds of method, namely first, change in frequency, second, the peak breadth in the internal friction curve. In this investigation, the activation energy was evaluated by this method of the change in the frequency using the following equation[15),16].

$$H = R*\ln(\omega_1/\omega_2)/(1/T_1 - 1/T_2) \quad (1)$$

H: Activation energy for hydrogen diffusion (J/mol)
R: Gas constant (mol/J/K)
T: Peak temperature (K)
ω: Amplitude (rad.) (= $2\pi f$)
f: Frequency (Hz)
τ: Period (= 1/f)

The internal friction measurement was performed by the specimen of length of 89 mm and 22 mm, the measurement is made three times each. As the results, τ and T was evaluated as 0.8687 and 80.79(K) respectively, for the specimen 89 mm long. For the other specimen, 0.4625, and 83.18(K) respectively. The activation energy was calculated based upon the results, and evaluated as 15000 J/mol. The activation energy was 23500 J/mol using Wert's equation[12].

These activation energy obtained in this investigation was in good agreement with that of hydrogen diffusion evaluated by Wasilewski[13], that is 27800 J/mol. Consequently, the peak at about 80 K is concluded to be Snoek peak of hydrogen in the β phase.

3.4 Hydride precipitation behavior in the $\alpha+\beta$ microstructure

As shown in Fig. 5, the relatively integrated intensity of β phase, α phase and γ hydride phase respectively changed by cathodic charging. Then the relation between volume fraction of the each phase and charging time was evaluated. Now, the volume fraction was evaluated from following equation[14].

$$\left.\begin{aligned} C_\beta &= (I_\beta/R_\beta)/S \\ C_\gamma &= (I_\gamma/R_\gamma)/S \\ C_\alpha &= 1-(C_\beta+C_\gamma) \end{aligned}\right\} \quad (2)$$

$$S = I_\alpha/R_\alpha + I_\beta/R_\beta + I_\gamma/R_\gamma$$

$$R = (1-v^2)\{|F|^2 \cdot P(1+\cos 2\theta)/(\sin\theta\cdot\cos\theta)\}\exp(-2M)$$

$C_\alpha, C_\beta, C_\gamma$: Volume fraction of each phase
θ: Bragg angle
F: Structure factor
P: Multiplicity factor
exp(−2M): Temperature factor
v: Volume of unit cell

This direct comparison method is of greatest metallurgical interest because it can be applied directly to polycrystalline aggregates.

Figure 9 indicates the relation between the volume fraction of each phase and hydrogen charging time. The temperature factor exp(−2M) was used the value evaluated by Averbach[11], the factor of the γ hydride phase was used as 0.75.

For high current density of 4200 A/m^2, the volume fraction first decreases with increasing the volume fraction of γ hydride phase and following the fraction of β phase decreases.

It means that first the hydride precipitate inside the α phase at the α/β interface and next in the β phase. In the case of 500 A/m^2, the volume fraction of α phase decreases with increasing the γ hydride phase, but the volume fraction of phase is remained constant.

It means that γ hydride phase precipitate inside the α phase near the α/β interface.

For the charging current of 50 A/m^2, γ hydride phase was hardly detected even if the specimens were charged for 50.4 ks.

Figure 10 shows the transmission electron micrographs of mill annealed specimen after charging at 500 A/m^2 for

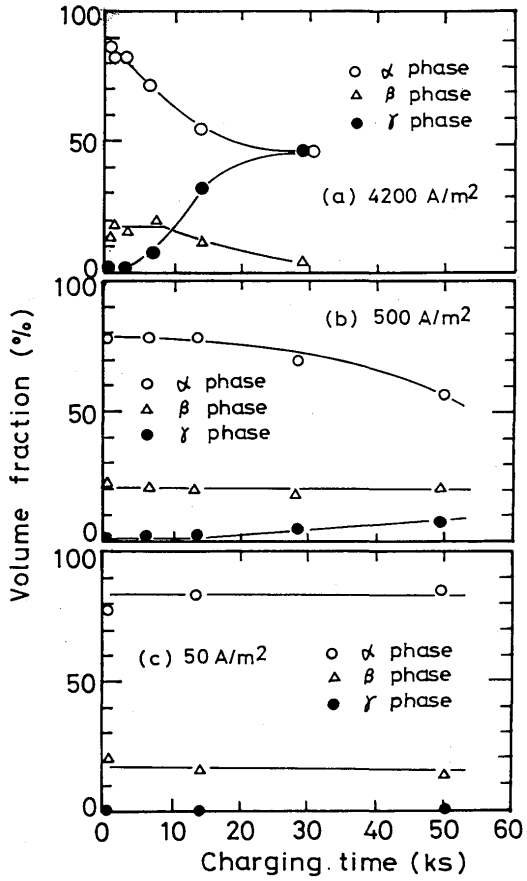

Fig. 9 Relation between volume fraction of α phase, β phase and γ hydride phase, and charging time for Ti-6Al-4V alloy by X-ray direct comparison method

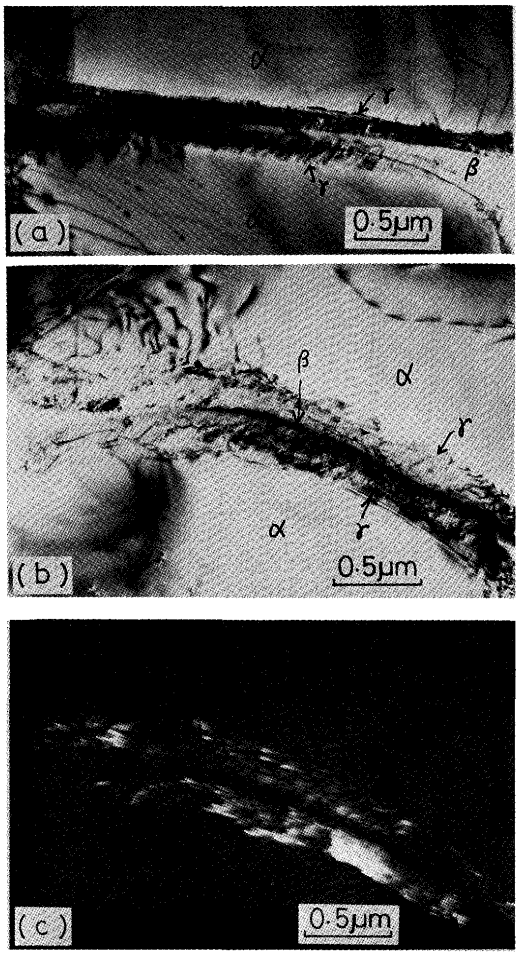

Fig. 10 Transmission electron micrographs of mill annealed specimen after charging at 500 A/m^2 for 3.6 ks
(a), (b): bright field image, (c): dark field image

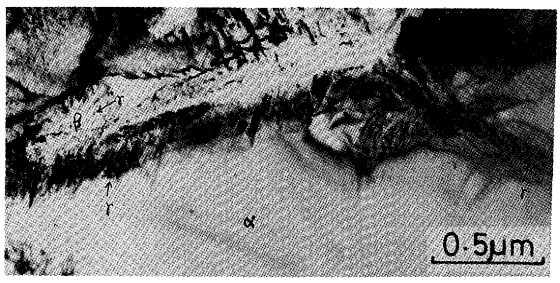

Fig. 11 Transmission electron micrographs of the specimen after charging at 4200 A/m^2 for 14.4 ks

3.6 ks.

As shown in Fig. 10-(a) and (b), γ hydride phase precipitates inside the α phase at α/β interface.

Figure 11 shows the transmission electron micrograph of the specimen after charging at 4200 A/m^2 for 14.4 ks. γ hydride phase precipitate not only inside the α phase at α/β interface but also in the β phase. The results are in good agreement with the results shown in Fig. 9.

For the current density of 4200 A/m^2, the fact that hydride precipitates in the β phase means that hydrogen concentration at the specimen surface is exceeded the solubility limit of hydrogen in the β phase. Consequently, as shown in Fig. 9-(c), that the decrease in the volume fraction of β phase revealed after 10 ks charging is considered as follows.

In the range of 2θ shown in Fig. 5, the effective X-ray penetration depth was 8 μm using Cu K_α, and then, if the hydride precipitate as the very thin layer near the surface, the hydride can be hardly detected by the X-ray method. For the internal friction measurement, hydrogen diffused inside the specimen through the β phase, the hydride can be detect not only near the surface but also inside the specimen.

Figure 12 indicates the relation between peak height at 190 K to 220 K and charging time for internal friction measurement shown in Fig. 6. The peak height increases with increasing the charging time and reaches a maximum constant value. This value depends on the current density of cathodic charging.

Consequently, this value is considered to be related to the volume fraction of the γ hydride phase, in the comparison of the results of X-ray volume fraction change

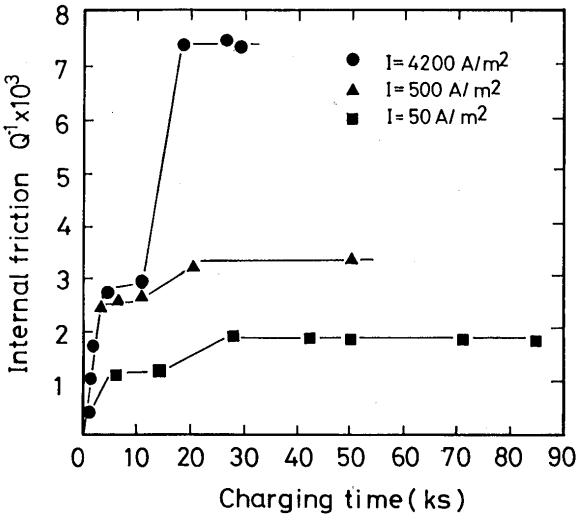

Fig. 12 Relation between peak height at 190 K to 220 K and charging time for internal friction measurement

shown in Fig. 9.

According to Someno et al[9], this peak is considered to be due to the stress induced diffusion of hydrogen in the hydride phase (fcc), namely he proposed that the peak at 200 K is due to the hydrogen movement from one tetrahedral site to another one, and the peak at 254 K is due to the hydrogen diffusion path from octahedral site to tetrahedral site.

This specimens were baked at 623 K in a argon atmosphere, and then measured the internal friction. This result is shown in **Fig. 13**. The peak at 190 K to 220 K and the

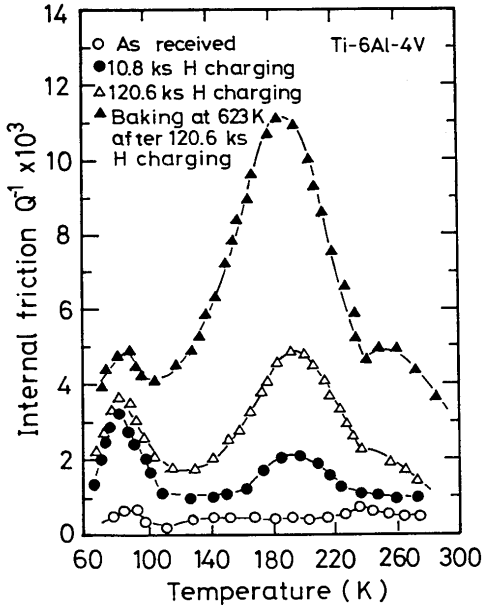

Fig. 13 Internal friction curves of Ti-6Al-4V alloys hydrogen-charged at 500 A/m² for various times, and then baked at 623 K

peak at 220 K to 260 K respectively extremely increases. It means that the hydride precipitates more by baking treatment. Consequently, the peak is concluded to be related to the hydride precipitation.

The change in microstructure with accompanies hydride precipitation leads to a large volume change of 17.2% for titanium[7]. Volume change of this magnitude cannot be accommodated elastically, this hydride precipitation requires plastic work accomplished by local deformation of the matrix at points adjacent to the hydride. The deformation results in the formation of dislocation. So, Tung[10] proposed that the peak is related to the interaction of hydrogen and dislocation.

4. Conclusion

An investigation has been made into the hydrogen diffusion and hydride precipitation behavior of $\alpha+\beta$ Ti-6Al-4V alloy cathodically charged at various current densities by means of X-ray diffraction method, internal friction measurement and transmission electron microscopy. The results obtained in this investigation are summarized as follows.

1) As $\alpha+\beta$ Ti-6Al-4V was cathodically charged, the diffraction peak of α phase by X-ray line profile was hardly shifted, but that of β phase was shifted to the low angle side.
2) d_{200} spacing of β phase increased with increasing the charging time and reached at a constant value. It means that hydrogen was mainly absorbed and diffusee to the β phase, and then solutionized up to the solubility limit.
3) The peak at about 80 K in the internal friction curve increases with increasing the charging time, and reaches at a maximum value at any current density. This peak is clear to be Snoek peak of hydrogen in the β phase. The tendency is in good agreement with the d_{200} change by X-ray diffraction line.
4) Based on the X-ray diffraction technique, the $\alpha+\beta$ Ti-6Al-4V showed the α phase and β phase peak before charging. But the new peak generated at 60.9 (π/180) rad., 92.8 (π/180) rad. so on, as the alloy was cathodically charged. The peak height increased with increasing the charging time and current density. It means that the peak is due to hydride precipitation.
5) The volume fraction of α phase decreased with increasing the precipitation of hydrides due to hydrogen charging at low current density, and that the hydrides precipitated in the α phase near the α/β interface is confirmed by transmission electron microscopy. In the case of high current density, the volume fraction in both α phase and β phase decreased with increasing the

volume fraction of γ hydride phase, detected the X-ray diffraction technique. It was confirmed that the hydrides precipitated both in the α phase near α/β interface and in the β phase, by means of transmission electron microscopy.

References

1) R.R. Boyer and W.F. Spurr: Met. Trans. A, 9A (1978), 23
2) J.L. Waisman, R. Trooky and G. Sines: Met. Trans. 8A (1978), 1249
3) D.A. Meyn: Met. Trans. 5 (1974), 2405
4) H.G. Nelson, D.P. Williams, and J.C. Stein: Met. Trans. 3 (1972), 469.
5) H.G. Nelson: Met. Trans. 7A (1976) 621
6) J.L. Waisman, G. Sines and L.B. Robinson: Met. Trans. 4 (1973), 291
7) G.F. Pittinato and W.D. Hanna: Met. Trans. 3 (1972), 2905
8) N.A. Tiner, T.L. Mackay, S.K. Asanmaa and R.G. Ingersoll: Trans. ASM, 61 (1968), 195
9) D. Someno, H. Nagasaki, and Y. Miyasaka: J. Japan Inst. Metal 8 (1967), 957 (In Japanese)
10) P.P. Tung and A.W. Sommer: Acta Met. 22 (1974), 191
11) B.L. Avervach, M.F. Comerford and M.B. Bever: Met. Trans. AIME 215 (1959), 682
12) C. Wert and J. Marx: Acta Met. 1 (1953), 113
13) R.J. Wasilewski and G.L. Kehl: Metallurgia 11 (1954), 225
14) Cullity: Elements of X-ray Diffraction, Addison-wesley Publishing (1978), 411
15) A.S. Nowick: Progress in Metal Physics, No. 5 (1953)
16) C. Zenar: Elasticity and Anelasticity of Metals (1948)